Original Article

Hepatic and Renal Ultrastructural Alterations Induced by Tamiflu on Male Rats

Wafaa H. Abdel-Ghaffar

Department of Zoology, Faculty of Science, Ain Shams University, Cairo, Egypt

ABSTRACT

Introduction: Tamiflu (T) is a brand-name antiviral drug. Many researchers have proven its efficacy in influenza treatment and prophylaxis. Meanwhile, other studies released reports on T, claiming that T is not efficacious for influenza treatment, but it just relieves some of the influenza symptoms; and induces some side-effects such as renal/psychiatric events, and serious heart rhythm problems. To stand on the truth between the aforementioned proofs and claims, this study was designed by applying the prescribed doses of T, which was announced by its manufacturer "Roche".

Study Design: Four animal groups (5 rats/each), in which the recommended doses were converted to rats. The control group (1st group), T-treated groups (6.75 mg/kg b.w.), where rats were given T twice in 5 days (2nd group), once in 10 days (3rd group), and once in 45 days (4th group). At the end, rats were rapidly dissected; the liver and kidney specimens were prepared for the TEM technique.

Results: The ultrathin sections of the affected hepatocytes of T-treated rats showed significant focal cytoplasmic degeneration/necrosis, which included: mega-mitochondria, marked dilatation of RER cisternae, cytoplasmic vacuolation, irregular nuclei with condensed heterochromatin, in addition to glycogen accumulation. The kidneys of the T-treated animals revealed serious changes: necrotic/ruptured epithelial cells of the renal corpuscles and disrupted foot processes. Swollen mitochondria were also seen in the epithelia of the proximal and distal convoluted tubules (PCTs and DCTs). The damaged BM and its lumen were occluded with degenerated and vacuolated ghost cells. The severity of the ultrastructural alterations was ascendingly graded as G III, II, then IV.

Conclusion: Finally, T induced hepatic and renal ultrastructure alterations in male rats. Such alterations match those enumerated by previous work that discover drug-induced liver/kidney injuries. So, it is recommended that T should be listed with drug-induced liver/kidney injury, as both alterations were observed on the obtained ultrastructural results.

Received: 29 January 2023, **Accepted:** 27 February 2023

Key Words: Mega-mitochondria, necrosis, renal corpuscles, RER, tamiflu.

Corresponding Author: Wafaa H. Abdel-Ghaffar, PhD, Department of Zoology, Faculty of Science, Ain Shams University, Cairo, Egypt, **Tel.**: +20 10 0750 6633, **E-mail:** wafaahassan@sci.asu.edu.eg

ISSN: 1110-0559, Vol. 47, No. 1

INTRODUCTION

In 1999, "Tamiflu" was launched as a brand antiviral drug with the generic name "Oseltamivir Phosphate (OP)", which is listed as a prophylactic drug for influenza in addition to its treatment. Its patency (1996) referred to Gilead Sciences and later was purchased by Hoffmann-La Roche (Roche) to develop and market the drug worldwide[1-2]. Indeed, more than 1042 journals published almost all data on OP concerned with its manufacturing, viability, treatment, or even with its side effects[3,4]. However, the papers concerned with the experimental trials of the drug to assess its side effects after administration whether to the humans[5-7] or experimental animals[8-22] are not sufficient. Despite all of these publications, no data could be taken as proof of the drug's efficacy. At the same time, during corona infection, drug usage in the treatment protocol was risky and physicians failed to depend on it during the pandemic infection of COVID-19. Due to this unclear and poor evidence to stand on the drug facts, and depending on previous studies done on the same issue[23], an essential need emerged to know the affected organelles inside the unit cells of the vital organs as liver and kidneys at the ultrastructure level because this field is almost rare in publications and recorded data.

MATERIALS AND METHODS

Chemicals and drug

TAMIFLU®/oseltamivir phosphate (75 mg, Figure A) is manufactured by F. Hoffman-La Roche, Gilead Sciences, Foster City, California, USA. The used drug form in this study is the orally-administrated capsules. All chemicals, solvents, and reagents utilized in the TEM method were of analytical and pure quality: Glutaraldehyde, Osmic acid (EMS, 2g), Xylene, Acetone (HPLC), ethyl alc. (HPLC), Hexane, Diethyl ether, Araldite kit (EMS), Sodium hydroxide, Paraformaldehyde, Formalin, Sodium citrate, Methanol, Ethyl acetate, Glass Knives (EMS), Carbon Coated mesh (200, EMS), Copper 200 mesh (EMS), Eppendorf, Falcon tubes (15cm & 50cm), Toluidine blue. In addition to laboratory supplies, yellow tips, blue tips, gloves, 50ml tightly-sealed wide plastic containers, 9cm glass petri dish, filter papers, and razors were also utilized.

 DOI: 10.21608/ejh.2023.174223.1815

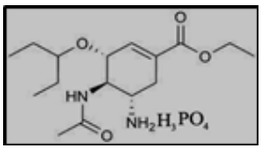

Fig. A: Oseltamivir phosphate

Animals

As an accommodation duration, twenty adult male albino rats (*Rattus norvegicus*) were placed in appropriate-sized cages at the Research Studies and Training Centre on Vectors of Diseases, Faculty of Science, Ain Shams University for two weeks. Water and normal pellets of animal feed were provided Ad libitum. To avoid any cross-contamination during the research time, nothing was left for coincidence; the animal partition upon which the entire research was conducted has been sterilized using the necessary detergent twice weekly. Changing and cleaning the animal cages were regularly done three times per week.

Experimental design and treatment schedule

The design of this experiment was based on 4 groups[22] (5 rats/each G). So, the total number of the used animals was twenty (4 Gs * 5 Rats = 20 Rats). The experimental rats were randomly allocated in suitable size cages after weighing, and were divided as follows:

Group I (G I): The control animals were given distilled water orally and on a regular basis.

All T-treated groups from G II to G IV received 6.75 mg/kg daily and orally[22], however, the period varied as follows:

Group 11 (G II): T was administered to the experimental animals twice daily for 5 days in a row. This kind of therapy is equal to the therapeutic dosage used in humans (75 mg/70 kg b. w. of T, twice orally/daily for 5 consecutive days).

Group III (G III): The rats were given T once a day for ten days. This medication is equivalent to the short-term preventive dosage used in people (75 mg/70 kg body weight of T orally/daily for 10 days).

Group IV (G IV): The animals were fed-T once a day for 45 days. This medication is equivalent to the long-term preventive dosage used in people.

All T-treated groups (II-IV) were administered in accordance with Lee *et al*., Hayden *et al*., and Peter *et al*.[23-25]; respectively. For the calculation of the above dosages and solution preparation to be suitable for oral administration by stomach tube, the protocol was applied according to Abdel-Ghaffar and Abdelghffar[22]. The dissection of the treated animals was done the day after the last dose per each group. Accordingly, the dissection was done on the 6th, 11th, and 46th day for animal groups 2, 3, and 4 respectively. All of the above-treated animals were anesthetized by using diethyl ether till death. The liver and kidney pieces were rapidly dissected to avoid post-mortem changes and prepared for the ultrastructural examination. Finally, after animal dissection, all of the biological wastes (solid waste; tissues and blood, etc.…) were collected in a fridge till being collected again to be burned at a Medical Waste Landfill (Incinerator) following the instructions previously announced by the Dean's Office of Faculty of Science, Ain Shams University.

Tissues sampling of the ultrastructural investigations

Specimen Preparation for Transmission Electron Microscopy "TEM" Investigations:

Liver and kidney samples were dissected as fast as possible and cut into small pieces for the ultrastructural studies. The specimens were immediately fixed in cold (4˚C) primary fixative composed of: 100ml formalin + 40ml glutaraldehyde (25%) solution + 2.7g NaOH + 11.6g NaH_2PO_4 dissolved in 1L distilled water overnight. Then, specimens were soaked in cold (4˚C) phosphate buffers for 3 h, followed by immersion in 2^{ry} fixative of Osmium Tetroxide (1%), dehydrated in ascending series of alcohol (15 min/each change, cold; 4˚C) started from 30%, 50%, 70%, till absolute alcohol. The latter change was done twice (30 min. for each change). Infiltration was done using a pure analytical grade of acetone (HPLC, Loba Chemie, twice, 30 min. for each change; at room temperature). Then subjected to a series of changes yielding hard rein capsules[26]. The polymerized resin blocks were trimmed and sectioned at 0.5 µm thickness using glass knives on an RMC ultramicrotome. Glass knives were used to cut silver and silver-gold ultrathin sections (70-90 nm in thickness) on the same ultramicrotome. The ultrathin portions were held in place by bare copper grids. Furthermore, transmission electron microscopy was used to study and photograph ultrathin sections stained with uranyl acetate and lead citrate (TEM, JEOL 1200 EX II Electron Microscope) at the E.M. Unit, at the Faculty of Science, Ain Shams University.

RESULTS

Ultrastructural findings of the liver

A normal hepatic cell and its organelles are illustrated in (Plate 1 Figures 1,2), which is limited with a plasma membrane. The liver cells are separated from the adjacent blood sinusoid(s) by a narrow perisinusoidal space that contains reticular fibres and is known as "the space of Disse" (Plate 1, Figure 2), and are lined with endothelial cells adjacent to a red blood cell. In the cytoplasmic part of the hepatocyte, the nucleus is continuous with the endoplasmic reticula. The latter is one of the most prominent cytoplasmic organelles, in addition to the mitochondria. The nucleus embodies prominent chromatin clumps and one or more nucleoli. The nucleus is prominent, centrally-located, almost spherical in shape, and is surrounded by a double-membraned nuclear envelope.

In T-treated groups, the degeneration was highly noticed in both groups; II and IV (Plate 1, Figures 3-4; and Plate 2. Figures 6-8, respectively), while in group

III the changes took place in a few cells (Plate 2, Figure 5). These affected hepatocytes showed focal cytoplasmic degeneration and necrosis. The cellular organelles became more condensed, poorly-defined (malformed), and the hepatocytes underwent more advanced degradation.

In group II: focal cytoplasmic necrosis and glycogen accumulation were recognized and associated with the accumulation of the RBCs in blood sinusoids (Plate 1, Figures 3,4). Although the findings of group "III" were the least among the treated groups in this study, by examining the affected cells; the cellular organelles of the endoplasmic reticula and mitochondria were found more condensed and deteriorated. In group IV: due to the intensive intake of T for 45 consecutive days, the examined hepatocytes showed numerous alterations; highly noticeable ballooning degeneration, dilatation of the cisternae of the rough reticula, and mega-mitochondria (Plate 2, Figures 6,9). In addition, burst hepatocytes that discharged all of their cellular contents in the surrounding with shrunken crenated nuclei were also seen (Plate 2, Figure 7). Finally, collagen fibres formed in between the boundaries of the degenerated cells (Plate2, Figure 8).

Ultrastructural findings of the kidneys

Group I: The glomeruli with its tuft of capillaries, basement membranes, endothelial cells, visceral epithelial cells with foot processes, glomerular capsules, mesangial cells, filtration slits, and intact clear urinary space are all visible in ultrathin sections of the kidneys of the control group (Plate 3, Figure 10). Proximal convoluted tubule from the same group also had intact basement membrane several mitochondria and spherical nuclei with proper chromatin distribution. Long microvilli (brush border) were seen normally directed towards the tubular lumen (Plate 3, Figure 11). Distal convoluted tubule of the control group had an intact basement membrane, small microvilli, spherical nuclei, and several well-intact mitochondria (Plate 3, Figure 12).

T-treated groups II, III, and IV

In **group II:** ultrathin sections of T-treated rats' kidneys demonstrated various modifications in the glomerular architecture (Plate 4, Figure 13). A part of the renal corpuscle showed necrotic epithelial cells with pyknotic nuclei, disrupted foot processes, and vacuolation. Proximal convoluted tubules exhibited several signs of degeneration (Plate 4, Figures 14-17). The epithelial cells were necrotic and darkened and were resting on damaged basement membrane. The tubule lumen is occluded with degenerated and vacuolated cells. The presence of dispersed enlarged mitochondria, as well as thicker and darker basement membranes, were also seen (Figure 16). Epithelial cells of these tubules were markedly ruptured (Plate 4. Figure 17). Also, the epithelial cells of the DCT lost their architecture and tubular organization. Variable nuclei, of the cells of the tubules, were obliterated (Plate 4, Figure 18).

Kidneys of group III exhibited the least degenerated changes among T-treated groups (Plates 5-7), with additional forms of changes. These changes included marked glomerular irregularity, with hypertrophied cells and vacuolated basement membrane (Plate 5, Figures 19-24). The endothelial cells and mesangial cells had pyknotic, as well as darken and shrunken nuclei (Figures 19,20). The basement membrane of the capillary lumen and visceral epithelial cells was markedly uneven, and the foot processes as well as the filtration slits were markedly damaged (Figures 21-24). Variable degrees of PCTs degeneration were also seen (Plate 6, Figures 25-30). Some PCTs cells exhibited pyknotic nuclei and numerous lysosomes, and others obliterated the tubular lumen (Figure 25). The apical part of a PCT showed multiple vacuoles along the base of its long microvilli (Figure 28). Also, the epithelial cells exhibited numerously swollen, and degenerated mitochondria with either partial or total destruction of the cristae (Figures 29,30). These changes were also associated with degenerated basement membranes. Variable necrotic epithelial cells of DCTs with degenerated nuclei that lost their normal architecture were seen. Also, the cytoplasm was loaded with numerous lysosomes that invaded the degenerated and vacuolated area (Figure 32). Other changes were the degeneration of the epithelial cells which possessed irregular nuclei, degenerated mitochondria and cytoplasmic vacuolation (Figure 33).

The examined ultrathin section of group IV showed more severe degradation than the above two groups which included: necrotic endothelial cells shrunken and hypertrophied visceral cells and shrunken Podocytes with shrunken and irregular disrupted foot processes (Plate 8, Figure 34). Parts of the renal corpuscles, including the parietal layer of Bowman's capsule, were detached, deteriorated, and accumulated with collagen fibres (Plate 8: Figures 35,36). In PCT, the lumen was obliterated with numerous ghost cells and necrotic dark epithelial cells with shrunken nuclei. Also, the intertubular capillary lumen was highly congested with red blood cells (Figures 37-39). Numerous degenerated DCTs, with dark, and necrotic epithelial cells were also seen (Plate 9: Figures 40-42). These alterations were associated with luminal obliteration with ghost cells and destruction of the tubular basement membrane. Numerous lysosomes, damaged mitochondria, dark cytoplasm, and most likely necrotic epithelial cells were also seen.

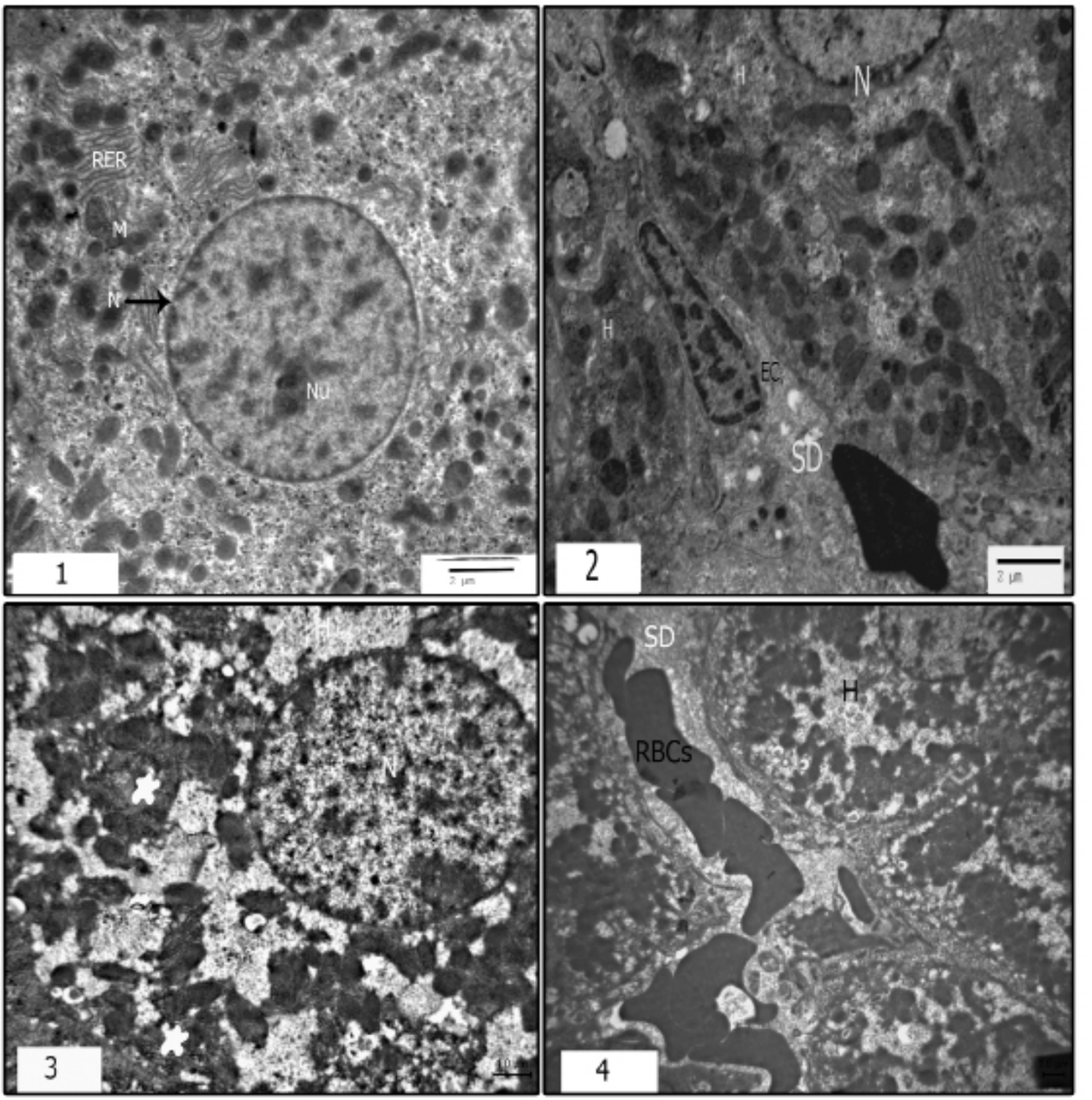

Plate 1 (Figs. 1-4): (Figs. 1 and 2): Electron micrographs of ultrathin sections of control rat liver showing 1): a part of a hepatocyte. In the cytoplasmic region, mitochondria (M), rough endoplasmic reticulum (RER), and a prominent nucleus (N) with a distinct nucleolus (Nu) are shown. X 8000. 2) the space of Disse (SD) and an endothelial cell (EC) are Shown. A red blood cell (RBC) is shown. X 4000. (Figs. 3 and 4): Electron micrographs of ultrathin sections of T-treated rats of group II showing :3) focal cytoplasmic necrosis and glycogen accumulation (*) 4): parts of 4 neighboring necrotic hepatocytes (H) with focal cytoplasmic degeneration with glycogen accumulation. The blood sinusoids are congested by RBCs. X 3000.

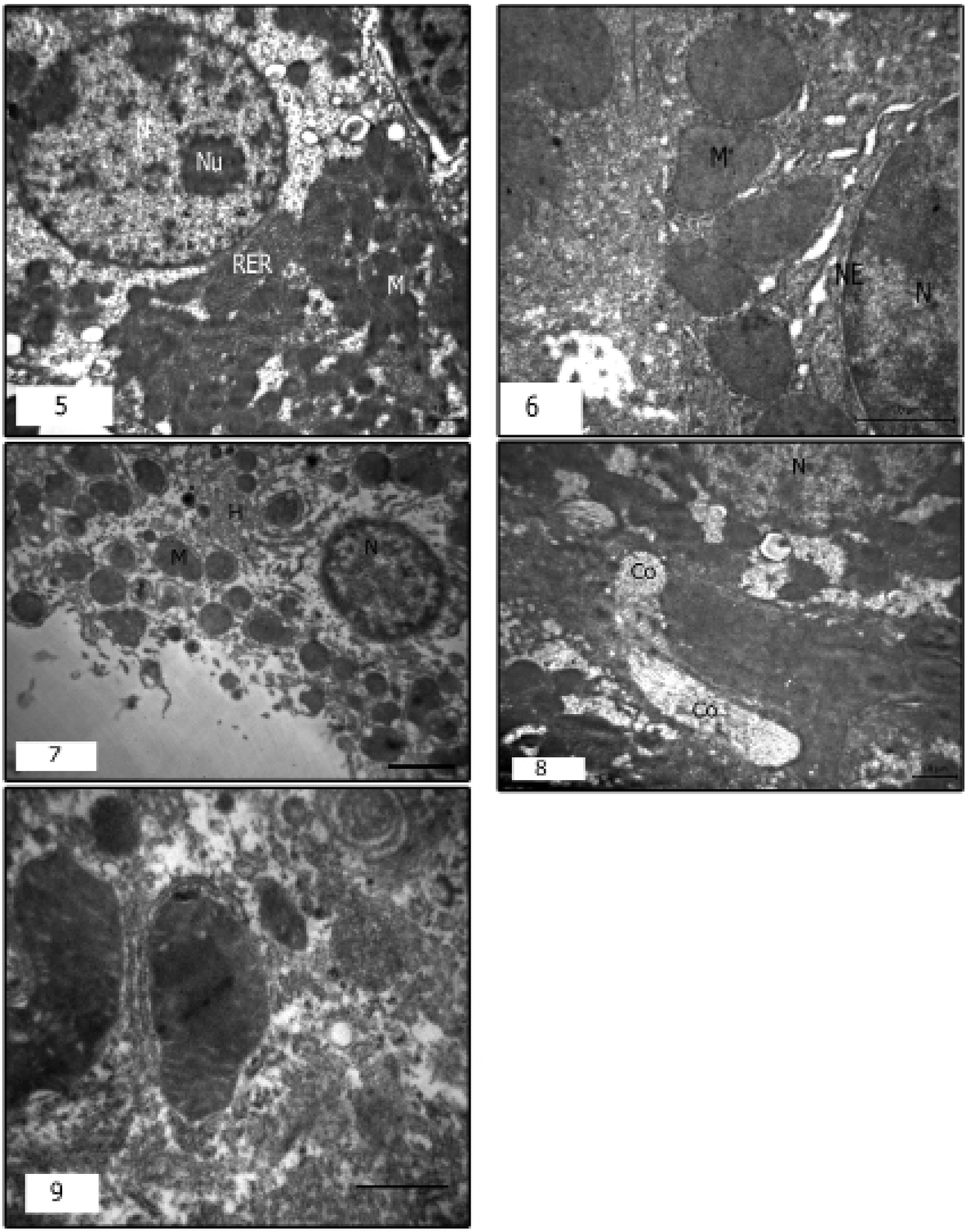

Plate 2 (Figs. 5-9): (Fig. 5) Electron micrograph of ultrathin section of T-treated rat of group III showing degeneration of RER and M, and numerous cytoplasmic vacuolation. X 8000 (Figs. 6-9) Electron micrographs of ultrathin sections of T-treated rats of group IV showing: 6) part of hepatocyte with ballooning degradation, widened RER cisternae, mega-mitochondria, and lysed cytoplasm. X 20000. 7) ruptured hepatocyte evacuates its cytoplasmic organelle and exhibits a shrunken N. X 10000. 8) emerged collagen fibres (Co) in between the degenerated hepatocytes. X 10000. 9) degenerated mega-mitochondria. X 30000.

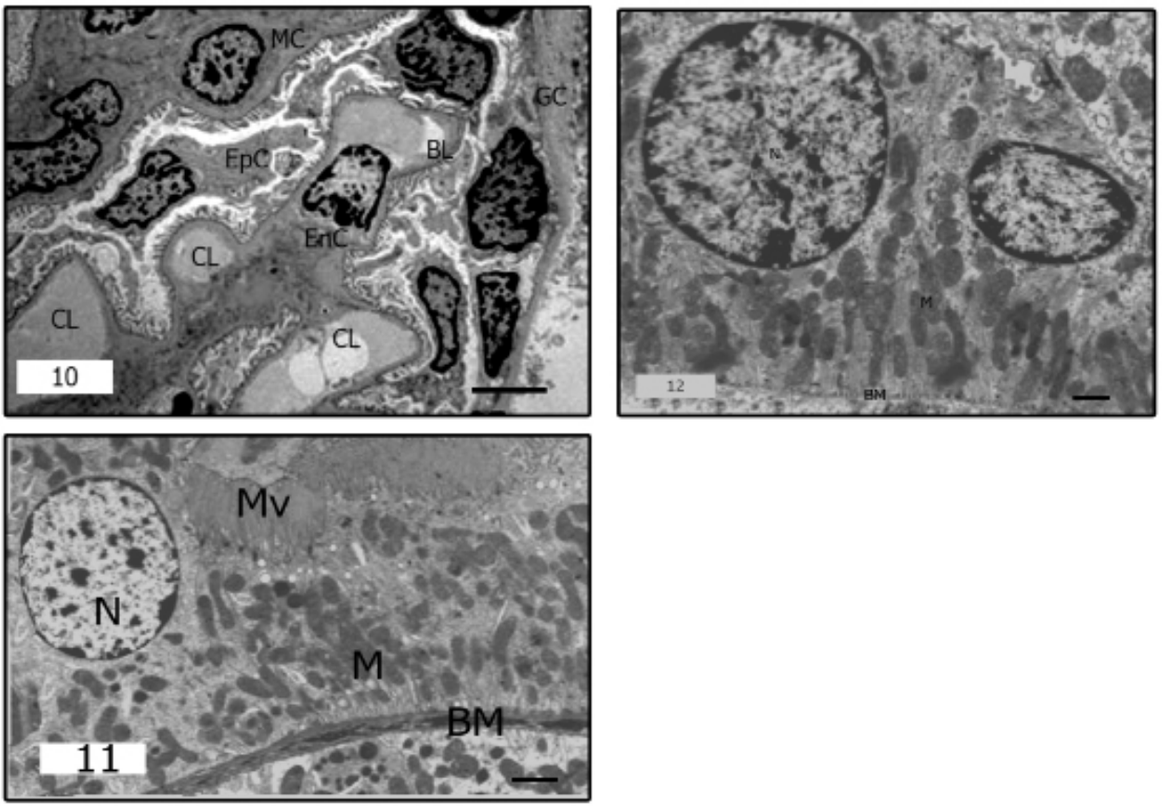

Plate 3 (Fig. 10-12): Electron micrographs of ultrathin sections of control rat kidney showing (10): the glomerulus and its capillary lumen (CL), a basement membrane, endothelial cell (EnC), a visceral epithelial cell (EpC) with foot processes, glomerulus capsule (GC) and mesangial cell (MC). (X 2000). (11): a proximal convoluted tubule epithelial cell resting on the typical structure of a basement membrane (BM). Notice, numerous intact mitochondria (M) and a round nucleus (N) with normal chromatin distribution. The apical surface shows normal long microvilli (Mv). X 7000 (12): a distal convoluted tubule epithelial cell resting on a basement membrane (BM). Notice, a round nucleus (N), and numerous intact mitochondria (M). X 5000.

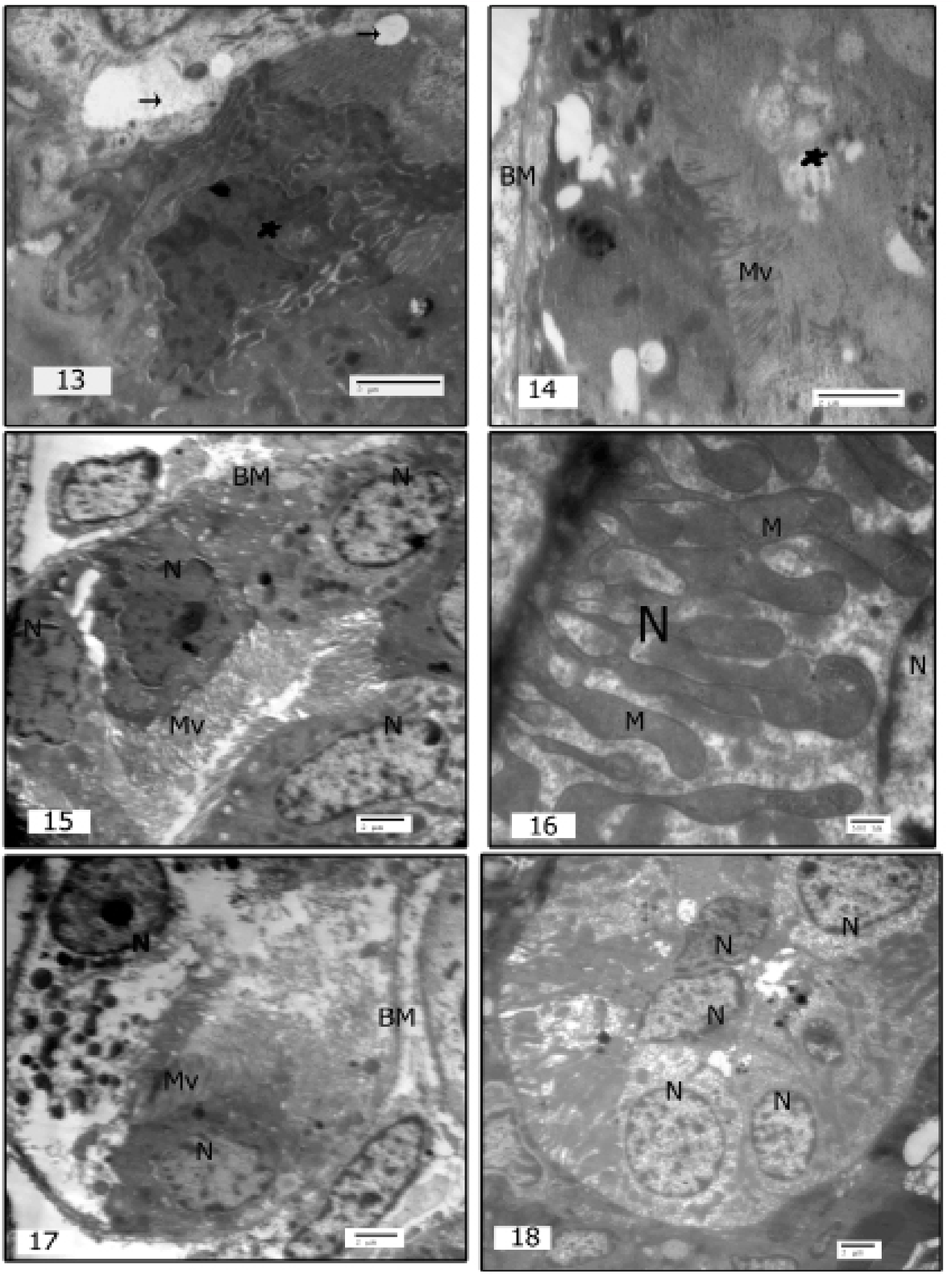

Plate 4: (Fig. 13-18). Electron micrographs of ultrathin sections of kidneys of T-treated rats of G II showing: 13) Changes of glomerular structures. A part of the renal corpuscle shows a necrotic epithelial cell (*) with a pyknotic nucleus, disrupted foot processes, and vacuolation (arrows). X 3000. (Figs. 14-17) represent numerous damaged PCTs. 14) showed a necrotic, darkened epithelial cell resting on a damaged BM. The tubule lumen is occluded with degenerated, and vacuolated cells (*). X 3000. 15) parts of several degenerated epithelial cells that lined the PCT with degenerated BM, and pleomorphic N. X 1500. 16) numerous scattered enlarged deteriorated M. 17) ruptured epithelial cells of PCT with degenerated BM, Mv, and N. 18) The epithelial cells of a DCT exhibit Pleomorphic N, lose their architecture, and tubular organization, in addition to cells obliterate its lumen. (X 2000).

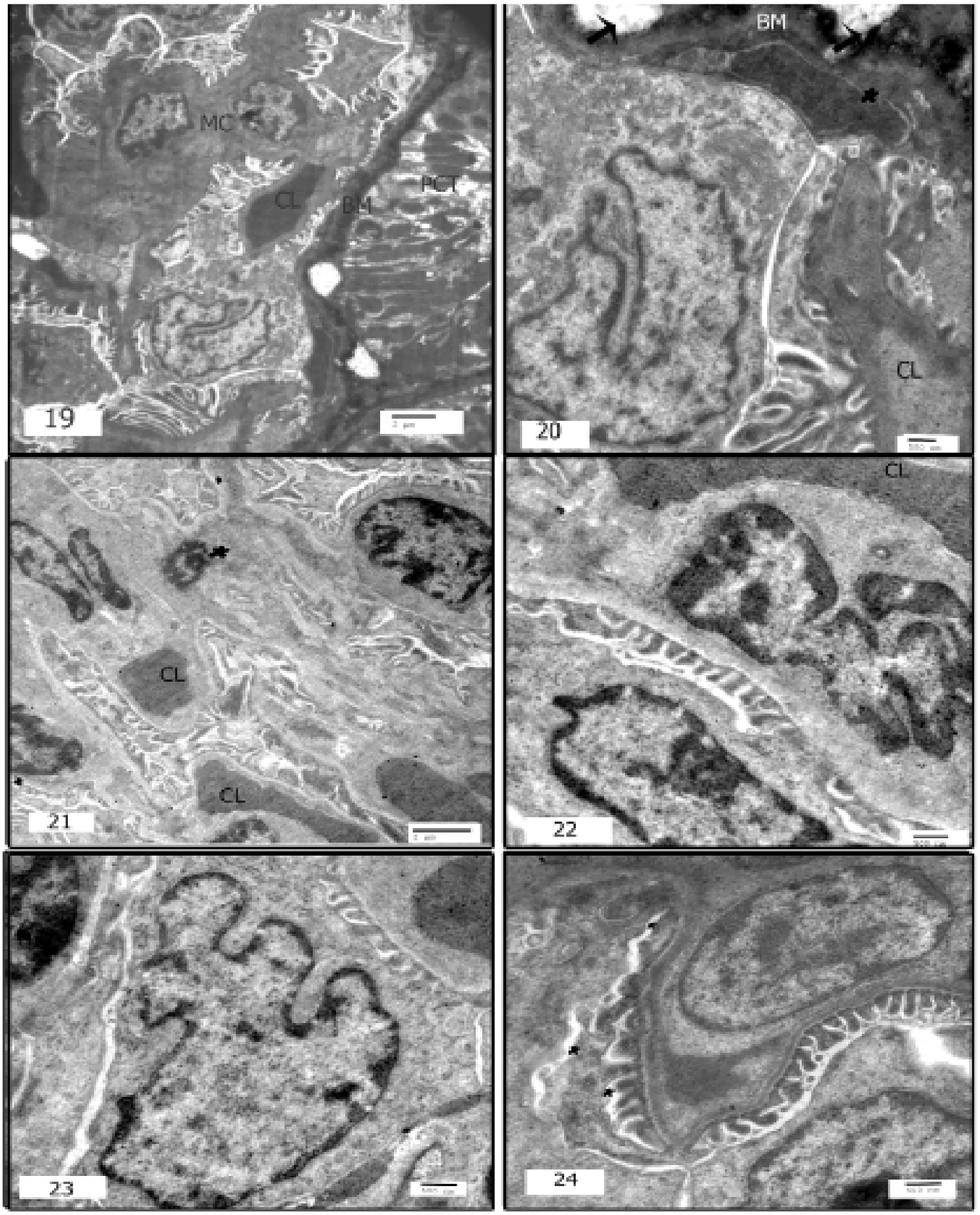

Plate 5: (Figs. 19-24). Electron micrographs of ultrathin sections of kidneys of T-treated rats of G III focus on the glomeruli and showing 19) marked irregularity, hypertrophied and vacuolated basement membrane (BM). The endothelial cells and mesangial cells in the capsular space show pyknotic, darkened, and other marked shrunken cells. A darkened part of PCT is shown. X 1500. 20) A magnified portion of Fig. 19 shows hypertrophied, vacuolated (arrow) basement membrane (BM), with pyknotic lining cell (*). A section of the glomerulus reveals its capillary lumen (CL) with significant basement membrane irregularity, a visceral epithelial cell exhibiting damaged foot processes, and filtration slits. X 4000. 21) shrunken nucleus of a visceral endothelial cell (*). X 2000. 22-24) visceral epithelial cells show variable degrees of disrupted foot processes and filtration slits. X 5000.

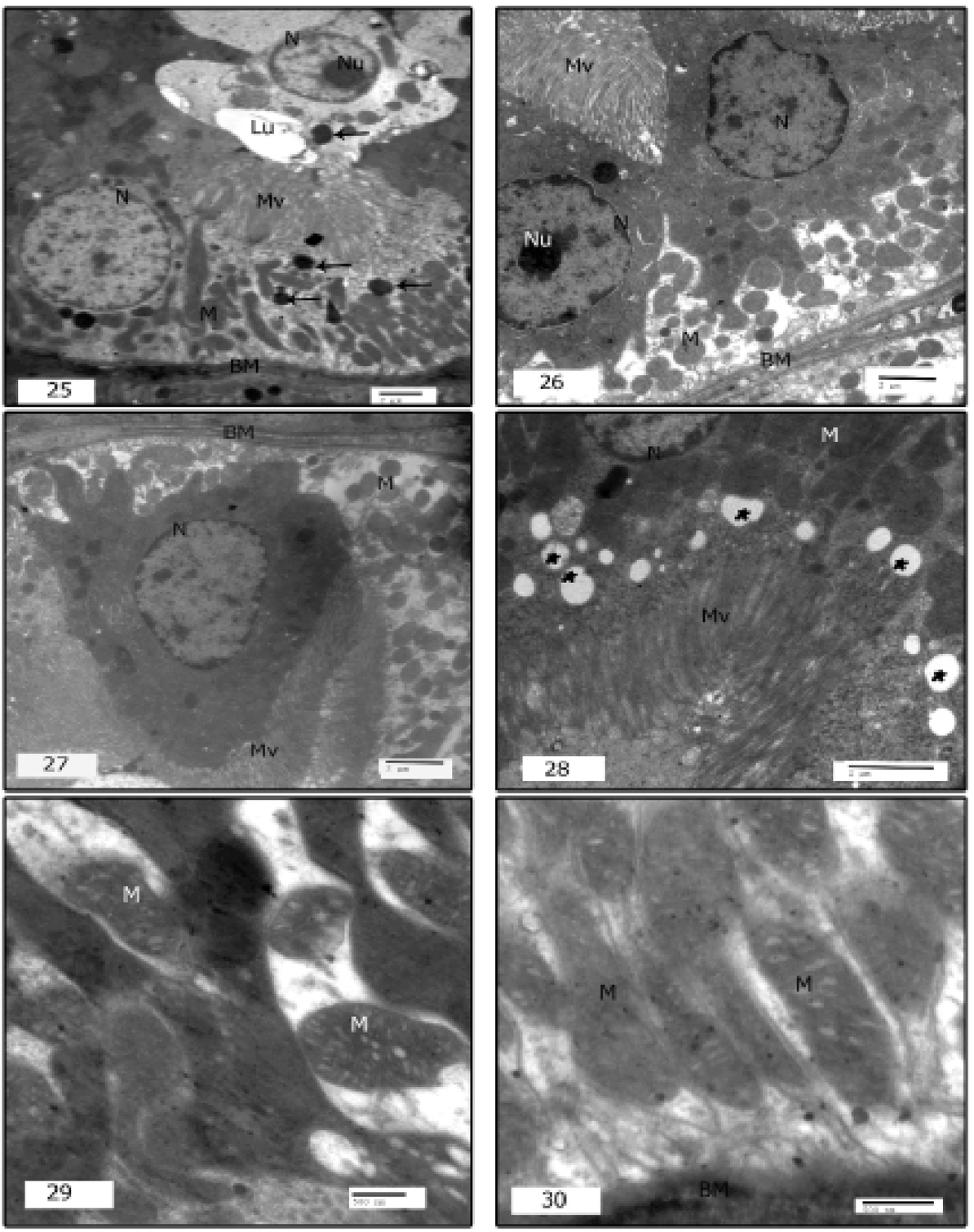

Plate 6: (Figs. 25-30). Electron micrographs of ultrathin sections of kidneys of T-treated rats of GIII focus on variable degrees of PCTs degeneration. 25) Pyknotic epithelial cells with numerous lysosomes (arrows). Other cells obliterate the tubular lumen (Lu). X 1500. 26 & 27) degenerated epithelial cells lose their intact to the degenerated basement membrane (BM). X 2000. 28) magnified apical part of a PCT showing multiple vacuoles (*) along the base of its long microvilli (Mv). X 3000. 29& 30) Magnified portions focused on the base of PCTs showing numerously swollen, and degenerated mitochondria (M) with partial and total destruction of the cristae. X 7500 & 10000.

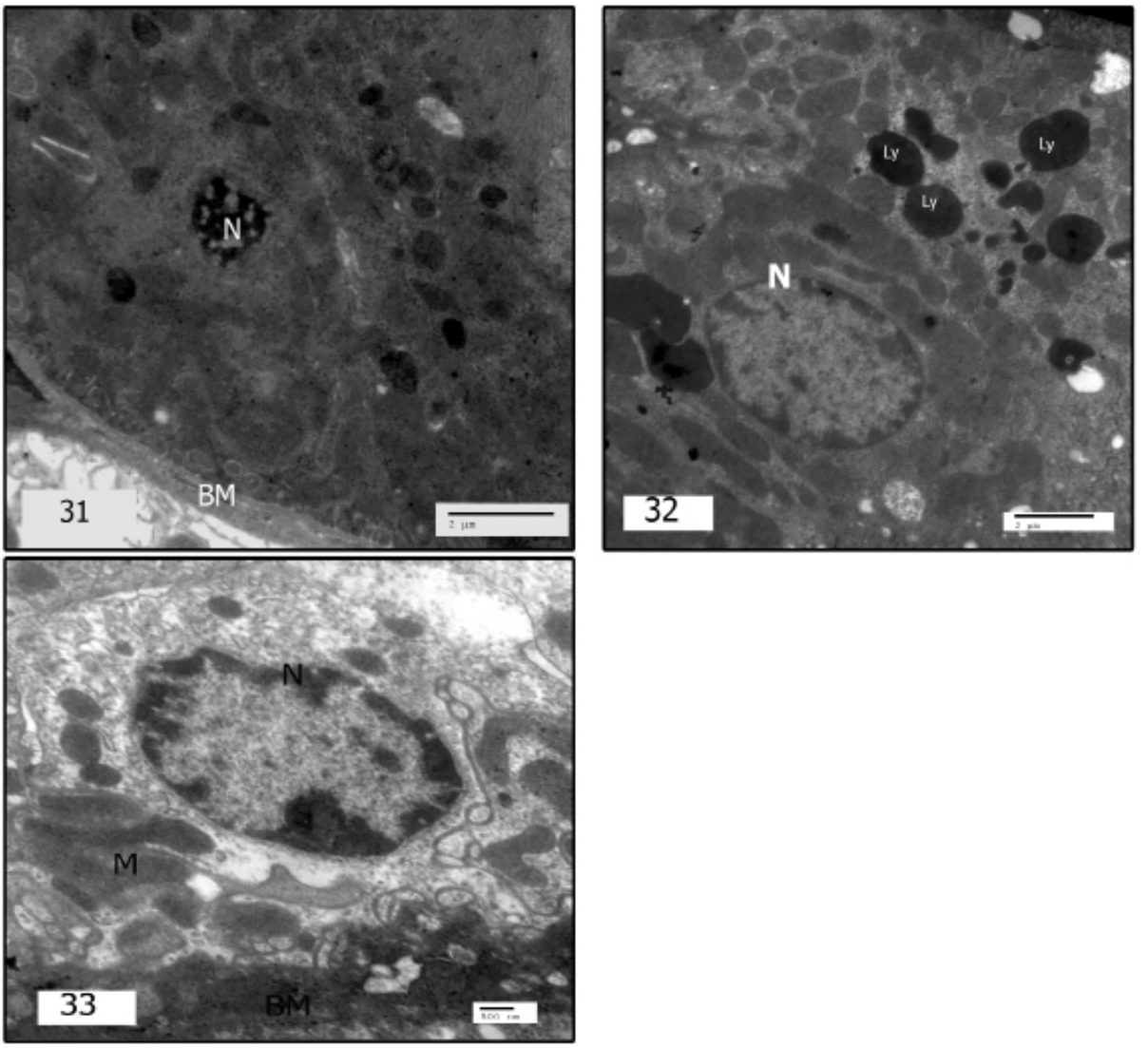

Plate 7: (Figs. 31-33). Electron micrographs of ultrathin sections of kidneys of Tamiflu-treated rats (G3, 6.75 mg/kg b. w. orally/ once-daily for 10 consecutive days) focused on Variable affected DCTs. 31) necrotic epithelial cell of DCT showing degenerated nucleus (N) that lost its normal architecture. X 3000. 32) An epithelial cell that is loaded with numerous lysosomes (Ly) invades the degenerated and vacuolated cytoplasm. X 2500. 33) another degenerated epithelial cell showing an irregular nucleus (N). notice the irrupted, degenerated cytoplasmic organelles including the mitochondria (M), and vacuoles. X 4000.

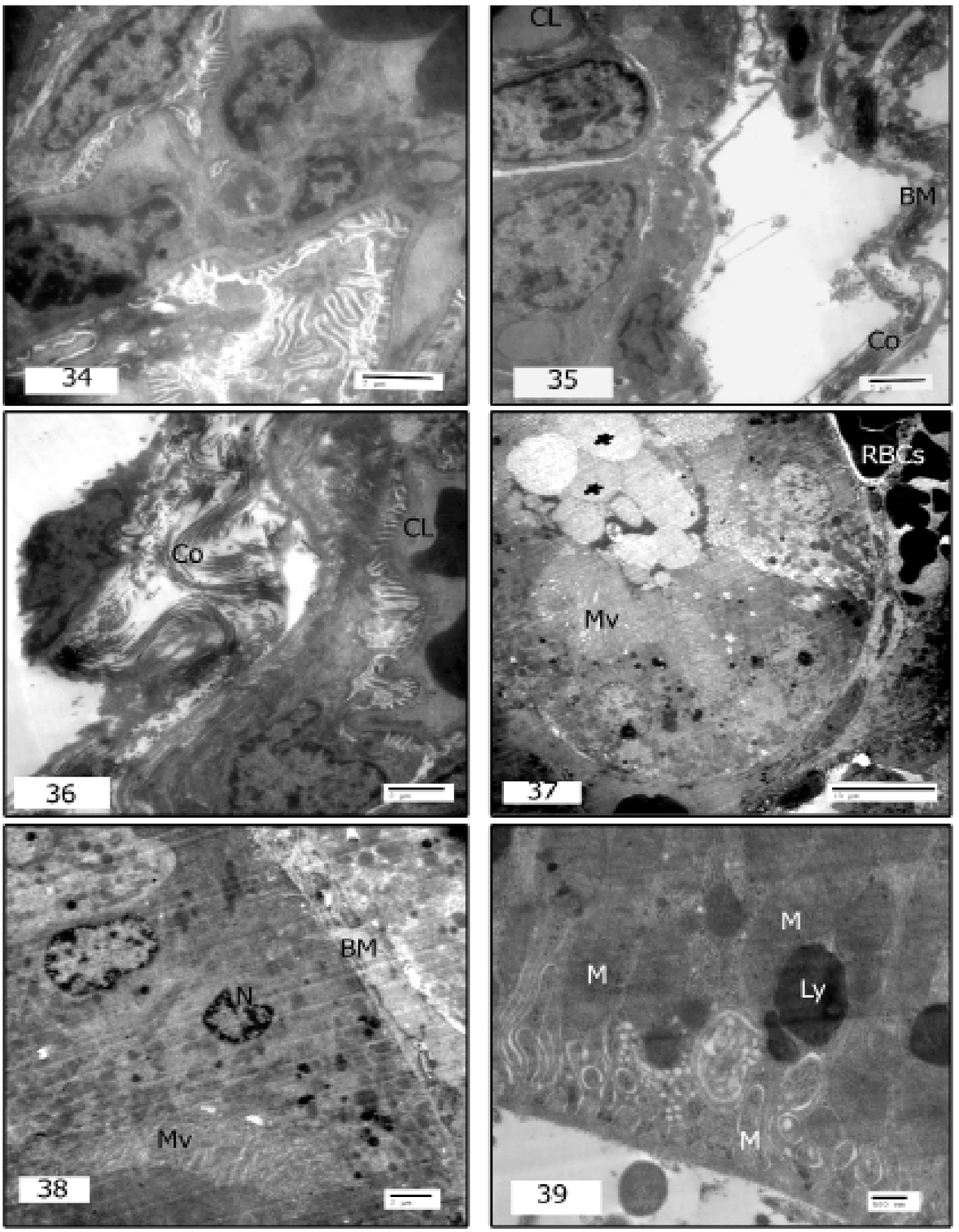

Plate 8: (Figs. 34-39). Electron micrographs of ultrathin sections of kidneys of T-treated rats of G4 showing 34) Part of a glomerulus with necrotic endothelial (shrunken/hypertrophied) visceral cells and degenerated shrunken Podocyte with shrunken irregular with disrupted foot processes. X 2500. 35 & 36) Parts of renal corpuscles, including the parietal layer of Bowman's capsule which is being detached and degenerated accompanied by collagen (Co) fibers formation. X 2000. 37) Part of PCT in which its lumen is obliterated with ghost cells (*). Notice the intertubular capillary lumen which is occluded by RBCs. X 750. 38) Two neighboring epithelial cells that represent part of DCT with their characteristic long Mv. Both cells are darkened and degenerated. Notice the shrunken nucleus towards the bottom of the micrograph. X 1500. 39) Magnified part of an epithelial cell of a PCT. The cell is invaded by lysosomes trying to scavenge the degenerated and swollen mitochondria (M). X 5000.

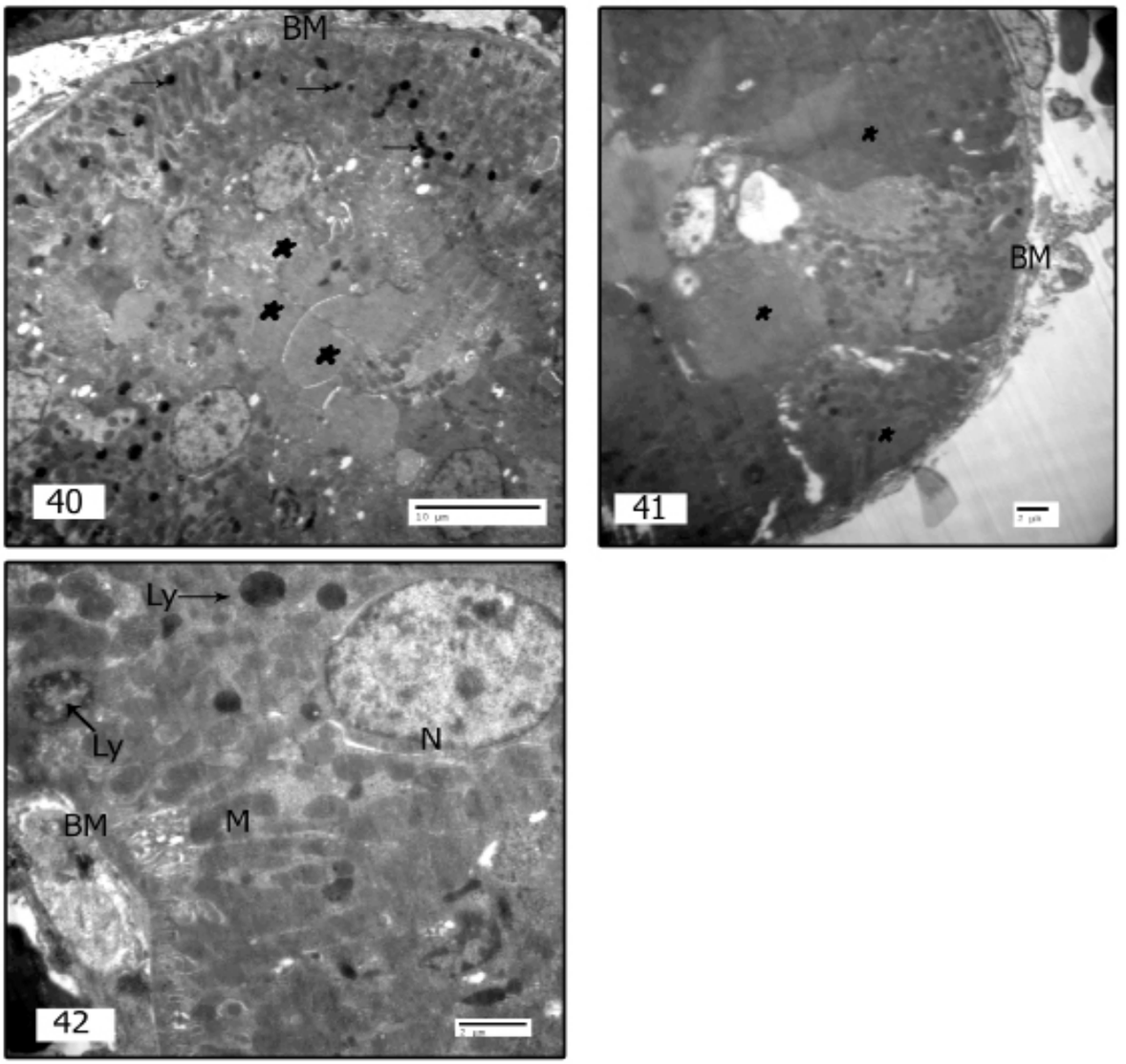

Plate 9: (Figs. 40-42). Electron micrographs of ultrathin sections of kidneys of T-treated rats of G IV showing DCTs. 40& 41) Parts of the degenerated, darkened, and necrotic epithelial cells form the PCTs. Notice that the tubules are obliterated with ghost cells towards the lumen of the tubules (*). In both Figs. the BMs are destructed. X 750 & 1000. 42) Magnified Part of the epithelial cell that lines a damaged DCT. Numerous lysosomes invade the cytoplasm of a darkened, necrotic epithelial cell with damaged M. X 2000.

DISCUSSION

No doubt that the whole world faced a disaster due to the pandemic consequences of COVID-19. During this unexpected catastrophe of the influenza pandemic, the physician had nothing to do except be the first line of defense and applied the information that they informed about the use of Tamiflu. T was the first choice for them in the treatment protocols[27]. The obtained shameful findings, during the pandemic, lead us to refer to the old publications that have criticized T since its inception[28-30].

The obtained ultrastructural observations from the present work revealed that the oral administration of T to male adult albino rats had induced moderate (as in GIII) and severe (as in GII & IV) alterations on both the liver and kidneys. Collectively, the ultrathin sections of the affected hepatocytes of T-treated rats showed significant alterations as hepatocytes focal cytoplasmic degeneration and necrosis, which included: mega-mitochondria (swollen mitochondria), ballooning degeneration, marked dilatation of RER cisternae, cytoplasmic vacuolation, nuclei with irregular nuclear envelope and condensed heterochromatin, in addition to glycogen accumulation. The kidneys of the T-treated animals revealed serious changes: necrotic and ruptured epithelial cells of the renal corpuscles and disrupted foot processes. Also, the PCTs' epithelia exhibited swollen mitochondria damaged BM, and their lumina were occluded with degenerated and vacuolated cells. Also, DCTs' epithelia lost their microvilli, and their lumina were obliterated with ghost cells. Referred to an atlas concerned with liver ultrastructure pathology, the authors literally illustrated several major and minor criteria that characterize drug-induced liver injury[31]. The authors stated that the presence of two or major criteria and combinations of major and minor criteria suggest that the drug owing toxic effects. In addition, minor criteria are most significant when extensive. The present study agreed with the aforementioned authors in the minor affected organelles criteria such as: vacuolation, mitochondrial changes, increase in lysosomes, glycogen accumulation, and cell necrosis, as well as in the major affected organelles criteria such as: the presence of mega-mitochondria, lysosomal invasion, and nuclear changes. Actually, more than 2 of the major and minor criteria were observed in the ultrathin sections of the present study that emphasize the abnormal ultrastructural alterations resulting from T-administration on both the liver and kidneys. Furthermore, the current study's findings are consistent with Ju *et al*[32] ideas of drug-induced liver harm. Also, the obtained results showed the effects of T on three variable durations, and the severity of the ultrastructural alterations becomes pronounced on the long duration due to dosages administration. This is the only research that examined the effect of treatment with variable dosages as well as Abdel-Ghaffar and Abdelghffar[22], and agrees with such findings.

The importance of the mitochondria as double membrane essential organelles is not only restricted to ATP production, but also in the cytosolic control of calcium[33,34]. In addition, mitochondria are involved in cell life/death and regulate cell apoptotic/necrotic death, so any alteration of the mitochondria may trigger cellular death[35,36]. The obtained results about mitochondrial alterations are in line with Al-Rikabi, Giovanni *et al*., and El-Alfy *et al*.[37-39,21].

In the ultrastructure observations of the kidneys, the cytoplasm of variable cells was full of variable forms of lysosomes as primary, 2ry, and tertiary lysosomes. Phillips *et al*.[31] stated that the lysosomes are involved in the metabolism or storage for numerous drugs. The lysosomal changes are always accompanied by focal cytoplasmic degeneration, the lysosomes become involved in the digestion of such damaged cytoplasmic portion[40,21]. It is worth noting that inflammatory cell buildup in the interstitial space has a pathogenic function in the development of tubular damage and interstitial fibrosis[41]. The authors hypothesized that PCTs facilitate interstitial macrophage infiltration due to their anatomic location and capacity to generate chemotactic cytokines, chemokines, and other inflammatory mediators of the epithelial cells.

All groups had abnormal endothelial basement membranes, hypertrophic endothelial cells in the capsular space, and visceral epithelial cells with damaged foot processes and filtration slits. Recent pathophysiological studies have revealed that the diffuse expansion of the mesangial region may play an important role in the obliteration of the capillary lumen, resulting in a reduction in the surface area available for filtration and, eventually, the cessation of glomerular function in various forms of glomerulopathy[42]. Furthermore, several glomeruli were atrophied with a dilated capsular space, which was consistent with the findings of a group of writers[43], who recognized this reduced glomerulus as sclerotic.

PCT epithelial cells exhibited loss of basal enfoldings and cytoplasmic vacuolation, as well as polymorphic swollen mitochondria and lack of functional long microvilli towards the capillary lumen. Furthermore, the DCT epithelial cells had enlarged mitochondria, a disrupted basement membrane, and a lack of microvilli. The basement membranes of the CTs seemed to deteriorate in general. Saadi *et al*.[44] interpret these indications as lipid peroxidation and the formation of free radicals, which degrade the lipid and protein structure of intracellular membranes and hydrolyze the cytoplasm. Nasr and Saleh[45] also observed nuclear alterations, damaged basement membrane with few basal enfoldings, swollen mitochondria, lysosomal invasion, and cytoplasmic vacuolation.

Finally, the causes of hepatotoxicity and nephrotoxicity caused by Tamiflu oral administration should be sufficiently focused on and carefully addressed by the authorized agents in charge of drug licensing. In addition, the license should not be given for market release if the manufacturer refused to furnish the documents of the concerned drug experimental trials. In this situation, Godlee[46] stated that Tamiflu, the medicine that cost the world billions of

dollars during the 2009 swine flu pandemic, demonstrated accessible evidence of inadequate, exaggerated, low-quality research supported mostly by pharma firms. During the COVID-19 pandemic, governments purchased massive supplies of Tamiflu and another medicine with no evidence to back up their purchase other than the manufacturer's biased released data that indicated "Tamiflu" cured all significant types of influenza, which resulted in a slew of bad outcomes.

Generally, Tamiflu oral administration induced ultrastructural hepato- and nephrotoxicity; hence, the presence of two or major criteria and combinations of major and minor criteria flare the priority to be listed as drug-induced liver and kidney injuries.

CONCLUSION

In conclusion, T-induced hepatic and renal ultrastructure alterations in male rats. Such alterations match those enumerated by previous work that discover drug-induced liver/kidney injuries. So, it is recommended that T should be listed with drug-induced liver/kidney injury as both alterations were observed on the obtained ultrastructural results.

ABBREVIATIONS

T: Tamiflu. **OP:** Oseltamivir Phosphate. **PCT(s):** Proximal Convoluted tubule(s). **DCT(s):** Distal Convoluted Tubules. **G(s):** Group(s). **M:** Mitochondria. **RER:** rough endoplasmic reticulum. **Nu:** nucleolus. **Co:** collagen fibres. **H:** hepatocyte(s). **SD:** Space of Disse. **RBC(s):** Red blood cell(s). **BM:** basement membrane. **BL:** Basal lamina. **MC:** Mesangial Cell. **PCT(s):** Proximal convoluted tubule(s). **DCT(s):** Distal convoluted tubule(s). **(Mv):** microvilli. **(CL):** Capillary lumen.

FUNDING

The Sector of Higher Studies, Ain Shams University (ASU), funded this work with 10000 Egyptian pounds to complete TEM photomicrographs. In addition, the chemicals and glassware were Freely-purchase from the chemical Stock-room at the Zoology Department, Faculty of Science, ASU.

AVAILABILITY OF DATA AND MATERIALS

The datasets supporting this article's conclusions are included.

Ethics approval and consent to participate. This study follows guidelines for the care and handling of experimental animals established by the ethical Committee belonging to the Higher Studies and Research Sector, Faculty of Science, ASU. For the purpose of the experimental design, animal accommodation, preventing contamination, animal way of dosing, sacrificing, and getting rid of the wastes; the protocol was approved and in accordance given the code: ASU-SCI/ZOOL/2022/9/1.

CONFLICT OF INTERESTS

There are no conflicts of interest.

REFERENCES

1. Hayden FG, Atmar RL, Schilling M, Johnson C, Poretz D, Paar D, *et al*. (1999a): Use of the selective oral neuraminidase inhibitor oseltamivir to prevent influenza. N. Engl. J. Med., 341 (18): 1336-1343.
2. Hayden FG, Treanor JJ, Fritz RS, Lobo M, Betts RF, Miller M, *et al*. (1999b): Use of the oral neuraminidase inhibitor oseltamivir in experimental human influenza: randomized controlled trials for prevention and treatment. JAMA, 282 (13): 1240-1246.
3. Russell RJ, Haire LF, Stevens DJ, *et al*. (2006). The structure of H5N1 avian influenza neuraminidase suggests new opportunities for drug design. Nature 443 (7107):45-9.
4. De Clercq E (2006). Antiviral agents active against influenza A viruses. Nature Reviews Drug Discovery 5(12):1015-25.
5. Li L, Cai B. Wang M, and Zhu Y (2003). A double-blind, randomized, placebo-controlled multicenter study of oseltamivir phosphate for treatment of influenza infection in China. Chin Med J (Engl); 116(1): 44-8. doi: 10.3901/jme.2003.06.044.
6. Shao L, Wu Y, Zhou H, Qin P, Ni H, Peng J, and Hou M (2015). Successful treatment with oseltamivir phosphate in a patient with chronic immune thrombocytopenia positive for anti-GPIb/IX autoantibody. Platelets;26(5):495-7. doi: 10.3109/09537104.2014.948838
7. Dawood FS, Jara J, Gonzalez R, *et al*. (2016). A randomized, double-blind, placebo-controlled trial evaluating the safety of early oseltamivir treatment among children 0-9 years of age hospitalized with influenza in El Salvador and Panama. Antiviral Res., 133:85-94.
8. Burger R A, Billingsley J L, Huffman J H, Bailey KW, Kim CU, and Sidwell RW (2000). Immunological effects of the orally administered neuraminidase inhibitor oseltamivir in influenza virus infected and uninfected mice. Immunopharmacol., 47: 45-52.
9. Hill G, Cihlar T, Oo C, Ho ES, Prior K, Wiltshire H, Barrett J, Liu B, and Ward P (2002). The anti-influenza drug oseltamivir exhibits low potential to induce pharmacokinetic drug interactions via renal secretion-correlation of in *vivo* and in *vitro* studies. Drug Metab. Dispos., 30(1): 13-19.
10. El-Tantawi HG (2007). Histological and histochemical changes of liver, kidney, and testis of albino rat after experimental application of oseltamivir phosphate (Tamiflu). J. Arab Soc. Med. Res. (JASMR), 2(1): 35-43.
11. Izumi Y, Tokuda K, O'Del KA, Zorumski CF, and Narahashi T (2007). Neuroexcitatory actions of Tamiflu and its carboxylate metabolite. Neurosci. Lett., 426(1): 54-58.

12. Llyushina NA, Hoffmann E, Solomon R, Webster RG, and Govorkova EA (2007). Amantadine-oseltamivir combination therapy for H5N1 influenza virus infection in mice. Antivir. Ther., 12: 363-370.

13. Morimoto K, Nakakariya M, Shirasaka Y, Kakinuma C, Fujita T, Tamai I, and Ogihara T (2007). Oseltamivir (Tamiflu) efflux transport at the blood-brain barrier via P-glycoprotein. Drug Metab. Dispos., 36: 6-9.

14. Freichel C, Prinssen E, Hoffmann G, Gand L, Beck M, Weiser T, and Breidenbach A (2009). Oseltamivir is devoid of specific behavioral and other central nervous system effects in juvenile rats at supratherapeutic oral doses. Int. J. Virol., 5(3): 119-130.

15. White N, Webster RG, Govorkova EA, and Uyeki TM (2009). What Is the Optimal Therapy for Patients with H5N1 Influenza? PLoS Med., 6(6): 1-6.

16. El-Sayed WM, and Al-Kahtani MA (2011). Potential adverse effects of oseltamivir in rats: males are more vulnerable than females. Can. J. Physiol. Pharmacol., 89: 623-630.

17. Abass AB, Abass DA, and Rasheed EM (2012). Neurotoxic effect in lactating mice pups received oseltamivir phosphate (Tamiflu) through milk from dosed nursing mothers during lactation period. Iraqi J. Vet. Med., 36 (1): 75-84.

18. Pourroy BN, Kolmos HJ, and Nielsen LP (2012). Antibody administration in experimental influenza increases survival and enhances the effect of oseltamivir. Health (Special Issue), 4: 933-940.

19. Abbas AB, Abass DA, Rasheed EM, and Khamas WA (2013). Evaluation of oseltamivir phosphate oral administration on selected organs during suckling period in mice pups. Bio. Life Sci., 4(1): 6-10.

20. EL-Ganzuri M, Hassab El-Nabi S, Saafan N, Abdel-Ghaffar WH (2016). Molecular studies of the effects of the antiviral drug, oseltamivir (Tamiflu), on the DNA of the testes' cells and the leucocytes of the male adult albino rats. Egypt. J. Zool.,65:159-184.

21. El-Alfy NZ, Sakr SM, Mahmoud MF, and Omar HA (2021). Effects of Tamiflu and Adamine on histology and ultrastructure of the liver of albino mice. Egyptian Liver Journal; 11(55): 1-21. https://doi.org/10.1186/s43066-021-00112-9

22. Abdel-Ghaffar WH, and Abdelghffar EA (2022). Pathophysiological effects of Tamiflu on liver and kidneys of male rats. Beni-Suef Univ J Basic Appl. Sci. 11(15): 1-14. https://doi.org/10.1186/s43088-021-00189-6.

23. Lee N, Chan PK, Hui DS, Choi KW (2009) Viral loads and duration of viral shedding in adult patients hospitalized with infuenza. J Infect Dis 200:492–500.

24. Hayden FG, Belshe R, Villanueva C, Lanno R, Hughes C, Small I, Dutkowski R, Ward P, Carr J (2004) Management of infuenza in households: a prospective, randomized comparison of oseltamivir treatment with or without postexposure prophylaxis. J Infect Dis 189:440–449.

25. Peters PH Jr, Gravenstein S, Norwood P, De Bock V, Van Couter A, Gib bens M, von Planta TA, Ward P (2001) Long-term use of oseltamivir for the prophylaxis of infuenza in a vaccinated frail older population. J Am Geriatr Soc 49:1025–1031.

26. Williams DB, and Carter CB (2009). Transmission Electron Microscopy: A Textbook for Materials Science. Springer Science and Business Media, LLC, 233 Spring Street, New York, NY10013, USA.

27. Choy KT, Wong AY, Kaewpreedee P, Sia SF, Chen D, Hui KPY, Chu DKW, Chan MCW, Cheung PP, Huang X (2020). Remdesivir, lopinavir, emetine, and homoharringtonine inhibit SARS CoV 2 replication in *vitro*. Antiviral Res 178:104786

28. Farina V, and Brown J D (2006). Tamiflu: The supply problem. Angew. Chem. Int. Ed. Engl.; 45(44). 7330-7334 doi:10.1002/anie.200602623.

29. Loder E, Tovey D, and Godlee F (2014). The Tamiflu trials "Progress towards data sharing but many battles still to fight". BMJ; 348: g2630.

30. Bulter D (2014). Epidemiology: Tamiflu report comes under fire "conclusions on stockpiling of antiviral drugs challenged". Nature; 508: 439-440.

31. Phillips MJ, Poucell S, Patterson J, and Valencia P (1987). The liver: An atlas and text of ultrastructural pathology. Raven Press, New York. USA.

32. Ju C, Reilly TP, Bourdi M, Radonovich MF, Brady JN, George JW, Pohl LR(2002). Protective role of Kupffer cells in acetaminophen-induced hepatic injury in mice. Chem Res Toxicol 15:1504–1513. https://doi.org/10.1021/tx02 55976 PMID: 12482232

33. Hatefi Y (1985) The mitochondrial electron transport and oxidative phosphorylation system. Annu Rev Biochem 54:1015–1069. https://doi.org/10.1146/annurev.bi.54.070185.005055 PMID: 2862839

34. Pozzan T, Magalhaes P, Rizzuto R (2000.) The comeback of mitochondria to calcium signaling. Cell Calcium 28:279–283. https://doi.org/10.1054/ceca.2000.0166

35. Starkov AA (2008). The role of mitochondria in reactive oxygen species metabolism and signaling. Ann N Y Acad Sci 1147:37–52. https://doi.org/10.1196/annals.1427.015 PMID: 19076429 PMCID: PMC2869479

36. Michael R, Duchen, Gyorgy S (2010) Roles of mitochondria in human disease. Biochem Soc 47:115–137. https://doi.org/10.1042/bse0470115 PMID: 20533904

37. Al-Rikabi FM (2012). Evaluation of selected parameters of rat liver injury following repeated administration of oseltamivir for diferent periods. Iraq J Vet Med 36(1):137–144

38. Al-Rikabi FM (2014). The Nephrotoxic Impact of Oseltamivir in Male Albino Rats after Repeated Exposure. Pharmacology & Pharmacy 5:479–486

39. Giovanni Q, Rosella S, Maria R, Francesca A, Darius M, Nazzareno C, Claudia P (2014). Protective role of amantadine in mitochondrial dysfunction and oxidative stress mediated by hepatitis C virus protein expression. Biochem Pharmacol 89: 545–556. https://doi.org/10.1016/j.bcp.2014.03.018 PMID: 24726442

40. Sakr SM (2007). Influence of tamoxifen on the liver of albino mice and the possible protective role of vitamin C. Egypt J Zool., 49:233–252 www. egyzolsoc.com.

41. Vielhauer V, Anders HJ, Mack M, Cihak J, Strutz F, Stangassinger M, Luckow B, Gröne HJ, and Schlöndorff D (2001). Obstructive nephropathy in the mouse: progressive fibrosis correlates with tubulointerstitial chemokine expression and accumulation of CC chemokine receptor 2- and 5-positive leukocytes. J. Am. Soc. Nephrol., 12(6):1173-87.

42. Quezada C, Alarcón S, Jaramillo C, Muñoz D, Oyarzún C, and San Martín R (2013). Targeting adenosine signaling to treatment of diabetic nephropathy. Curr. Drug Targets; 14(4):490-6.

43. Markowitz GS, Radhakrishnan J, Kambham N, Valeri AM, Hines WH, and D'Agati VD (2000). Lithium nephrotoxicity: a progressive combined glomerular and tubulointerstitial nephropathy. J. Am. Soc. Nephrol., 11(8):1439-48.

44. Saadi, L.; Lebaili, N. & Benyoussi, M (2008). Exploration of cytotoxic effect of Malathion on some rat organs structure. Commun. Agric. Appl. Biol. Sci., 73(4):875-81.

45. Nasr AY, and Saleh HA (2014). Aged garlic extract protects against oxidative stress and renal changes in cisplatin-treated adult male rats. Cancer Cell Int., 14(1):92.

46. Godlee F (2020): Covid-19: The lost lessons of Tamiflu. BMJ, 371: m4701.

الملخص العربى

"التغييرات التركيبية الدقيقه الكبدية والكلوية المستحثة باستخدام عقّار التاميفلو على ذكور الجرذان"

وفاء حسن عبدالغفار

قسم علم الحيوان، كلية العلوم، جامعة عين شمس، القاهرة، مصر

الخلفية: تاميفلو "T" دواء مضاد للفيروسات يحمل علامة تجارية. لقد أثبت العديد من الباحثين فعاليته في علاج الأنفلونزا والوقاية منها. في غضون ذلك ، نشرت دراسات أخرى تقارير عن عقار تاميفلو زعمت أن عقار تاميفلو غير فعال في محاربة الإنفلونزا ولكنه يخفف فقط من بعض أعراض الإنفلونزا. وتسبب في ظهور بعض الآثار الجانبية الكلوية/النفسية ، ومشاكل خطيرة في ضربات القلب. وللوقوف على الحقيقة بين الإثباتات والادعاءات السابقة ؛ على التوالى. تم تصميم هذه الدراسة من خلال تطبيق الجرعات الموصوفة من التاميفلو، والتي تم الإعلان عنها من قبل الشركة المصنعة (روش).

تصميم الدراسة: أربع مجموعات حيوانية (٥ جرذان/كل مجموعة) ، تم تحويل الجرعات الموصى بها إلى الجرذان. المجموعة الضابطة (المجموعة الأولى) ، المجموعات المعالجة بـالتاميفلو (٦,٧٥ مجم من التاميفلو / كجم من وزن الجسم): تلقت الجرذان التاميفلو مرتين لمدة ٥ أيام متتالية (المجوعة الثانية)، ومرة واحدة لمدة ١٠ أيام (المجموعة الثالثة) و ٤٥ يومًا (المجموعة الرابعة). في النهاية، تم تشريح الجرذان بسرعة وتم تحضير الأنسجة (عينات الكبد والكلى) لتقنية الميكرسكوب الضوئى النافذ.

النتائج: أظهرت المقاطع شديدة الرقة للخلايا الكبدية للجرذان والمعالجة بالتاميفلو تغيرات ملحوظة مثل تنكس/تنخر سيتوبلازمى بؤرى, كما شملت: تضخم الميتوكوندريا وتضخم و توسع ملحوظ في الشبكة الأندوبلازمية الخشنة، فجوات سيتوبلازمية ، نواة غير منتظمة مع تكدس الكروماتين, وتراكم الجليكوجين. أظهرت الخلايا الكلوية للحيوانات المعالجة بالتاميفلو تغيرات خطيرة: تمزق/ نخرالخلايا الطلائية لكريات ملبيجى. كما أظهرت تلف الخلايا الطلائيه المبطنة للانيبيبات الملتفة القريبة ، والتى تحوى ميتوكوندريا متورمة. كما أظهرت تلف الخلايا الطلائيه المبطنة للانيبيبات الملتفة البعيدة وتم أنسداد التجويف الخاص بهم بخلايا شبحية متدهورة ومفرغة. أيضا، شدة التغيرات التركيبية الدقيقة تتدرج من المجموعة ٣ ثم ٢ وبليها ٤.

الخلاصة: أخيرًا ، تسبب التاميفلو فى تغيرات تركيبية دقيقة بذكور الجرذان. وتتطابق هذه التغيرات مع ماتم نشرة فى أبحاث سابقة تتضمن قائمه بها العديد من الأدوية المحدثة للتلف بالكبد / والكلى. لذلك ، يوصى بإدراج التاميفلو ضمن تلك القائمة للأدوية التى تسبب تلف محدث بالكبد / والكلى.